Archive of SID.ir



Pages: 110-124 / Vol. 17 / Issue 2 / Summer-Fall 2024

Journal of Aerospace Science and Technology

Journal Homepage: https://jast.ias.ir

Original Research Article

The New Hybrid Meta-Model by Using DOE and RSM for Liquid Propellant Engine's Feed System Optimization

Hamid Reza Alimohammadi[1], Hasan Naseh[2*] and Fathollah ommi [3]

1,3- Aerospace Research Institute, Ministry of Science, Research and Technology, Tehran, Iran
2- Department of Mechanical Engineering, Tarbiat Modares University, Tehran, Iran

ARTICLE INFO

Received: 24 October 2022
Revised: 18 December 2023
Accepted: 27 December 2023
Available online: 27 December 2023

KEYWORDS:

New Hybrid Meta-Model,
Liquid Propellant Engine (LPE),
Feed System,
Design of Experiment (DOE),
Response Surface Method (RSM).

ABSTRACT

The present paper strives to optimize the feed system of the liquid-propellant engine (LPE). To this end, the new hybrid meta-model methodology by utilizing the Design of Experiment (DOE) method and the Response Surface Method (RSM) was developed and implemented as two effective means of designing, analyzing, and optimizing. The input design variables, constraints, objective function, and their surfaces were identified. Then, the design and development strategy was clarified by utilizing the combination of RSM, DOE, and regression analysis. Hence, 64 different experiments were carried out on the RD-253 propulsion system. The response surface curves were drawn, and the related objective function equation was obtained. The Analysis of Variance (ANOVA) results indicate that the developed hybrid model is capable of predicting the responses adequately within the limits of input parameters. In addition, the precision of the model was assessed by comparing it with the existing samples, and the output was interpreted and analyzed, which showed high accuracy. Hence, desirability function analysis has been applied to LPE's feed system to maximize the power and minimize the weight, simultaneously. Finally, confirmatory tests have been conducted with the optimum parametric conditions to validate the optimization techniques. In conclusion, the methodology capability is to optimize the LPE system, a 13 % increase in the power to feed system weight ratio and a 2% increase in the thrust to engine weight ratio. These values are considerably large for LPE design.

DOI:
https://doi.org/10.22034/JAST.2023367044.1135

1. INTRODUCTION

For aviation transportation, propulsion systems have received a great deal of attention, and practical applications are emerging in the optimization of the design of space systems, including the propulsion subsystems [1–8]. The effect of oxidizer-to-fuel mass ratio on dry and wet mass, specific impulse, propellant volume, and combustion chamber mass is impressive in comparison with chamber pressure and nozzle expansion ratio [9]. Saqlain and He [10] provided an efficient GA for the design of a liquid propellant space propulsion system. Minimizing the take-off mass was the objective function. The combustion chamber pressure, nozzle outlet pressure, chamber diameter, thrust, and burning

* Corresponding Author's Email: hnaseh@ari.ac.ir

Print ISSN:1735-2134 **Online ISSN:** 2345-3648

Archive of SID.ir

Archive of SID.ir

time were considered design variables. Jones [5] used a particle swarm optimization algorithm to optimize the specific impulse using the oxidizer-to-fuel mass ratio and nozzle expansion ratio. His approach used design optimization of the propulsion system, considering propellant combination, chamber pressure, and ambient pressure as input. Shafaee et al. [11] proposed a mass-based model to improve space propulsion systems' geometrical and performance parameters. They investigated a mass-based model for the optimization process. Their method used a hybrid GA sequential quadratic programming as an optimizer. The mass-based formulation problem was solved using a hybrid optimization algorithm with a GA as the global optimizer and sequential quadratic programming as the local optimizer, starting from the solution given by the GA. Xuan and Lam [12] studied multidisciplinary design optimization using the response surface method, GA, and simulated annealing. The article developed a novel framework for multidisciplinary design optimization. In terms of optimization algorithms, RSM, GA, and simulated annealing are utilized to get the global optimum.

Soldà [13] proposed a new feed system for LPE based on the use of electric pumps, whose power was supplied using batteries. This new feed system was named the electro-pump. In a study, these researchers demonstrated that the new system is a good alternative to the absolute blow feed system. Rachov and Tacca [14] indicated that the LPE with an electro-pump feed system is a suitable alternative to its former generations (i.e., the absolute blow and turbo-pump feed system). This study also compared turbo-pump feed systems with the absolute blow system. Moreover, it was indicated that the proposed system is even more effective in some applications than the turbo-pump feed system. It was also indicated that due to the use of this propellant technology in the lightweight space carriers, the space carrier has mass-wise superiority.

Moosavi [15] studied multi-level optimization of a centrifugal compressor. In this research, multi-level optimization of the profile of the splitter blades of a turbocharger compressor is performed using GA in order to improve its performance.

Mojaddam and Pullen [16] studied the optimization of a centrifugal compressor using the DOE Technique. Applying a novel approach to the problem, a complete factorial analysis was used to investigate the most effective parameters. The RSM was implemented to construct models and to recognize the best points over a design space created based on the Box-Behnken methodology. Lei et al. [17] proposed a multidisciplinary design optimization of the cooling turbine blade. The thickness of the blade wall, the thickness, and the height of ribs are chosen as design variables.

From the literature, it was seen that there is limited work on LPE's feed system Parameters. In addition, there is limited work on optimizing the input pressure of the oxidizer pump as well as the input pressure of the fuel pump, gas generator temperature, turbine efficiency, rotational speed, pump efficiency, and inlet relative cross-section. Hence, in the present work, an attempt has been made to optimize a bi-propellant LPE's feed system using the new hybrid meta-model methodology by utilizing the DOE and RSM with the aim of simplifying a complicated system such as the feed system. In addition, the interactions among the requirements are revealed, and the design precision and velocity are improved. The novelty aspect of the present study focuses on the development of computational as well as empirical models and multi-response parametric optimization in the LPE's feed system. Particularly, DOE and RSM have been applied to process improvement.

2. FEED SYSTEM INTRODUCING

In this study, the optimization problem is an RD-253 engine feed system. This engine was designed and manufactured from 1961 to 1965 for utilizing in stage one of the Proton-K space launch system in the design department of the Saint Petersburg (the former Soviet Union) gas dynamics laboratory. The pneumo-hydraulic circuit of this engine is depicted in Fig. (1) the type of propellant (fuel and oxidizer) in the engine used unsymmetrical di-methyl hydrazine, "$(CH_3)_2N_2H_2$" and di-nitrogen tetroxide, N_2O_4, respectively. The type of engine cycle utilized is from a closed-cycle. Fig. (2) illustrates the design functions of the RD-253 engine feed system. The design functions of the analyzed engine feed system in this study are as follows: the system, the main turbine, the main fuel pump, the pre-burner kick pump, the main oxidizer pump, and the pre-burner.

Table (1) presents the most important engine design requirements in this study. These

Archive of SID.ir

Archive of SID.ir

requirements include the propellant type, operating characteristics, environmental conditions, and physical requirements, which are provided in 12 rows. The values listed in the table present the operating conditions of the engine in the mentioned regime.

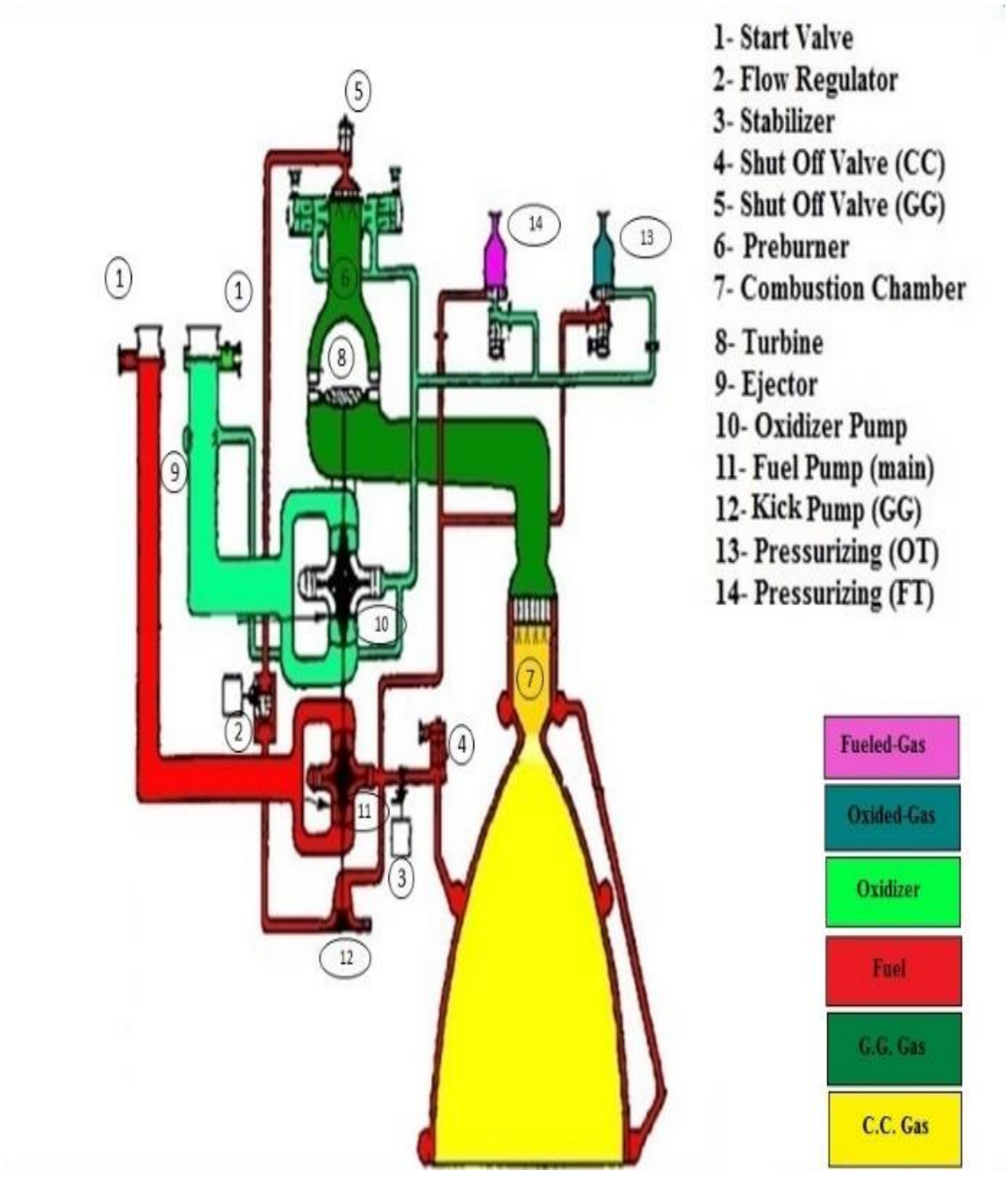

Fig. 1. The schematic of the RD-253 closed-cycle LPE.

Archive of SID.ir

Archive of SID.ir

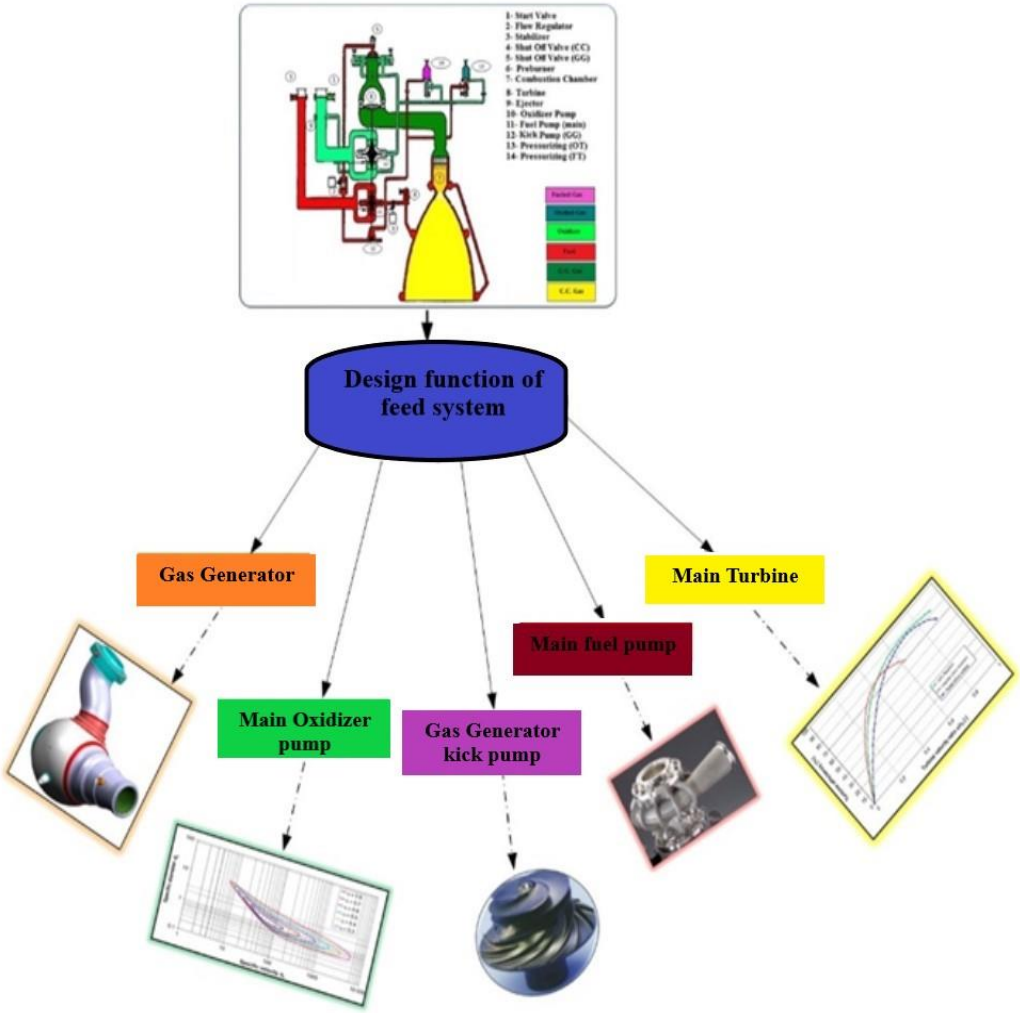

Fig. 2. The design functions of the RD-253 closed-cycle LPE feed system.

Table 1. The design requirements of the RD-253 LPE.

Requirements	Kind of Requirements	Unit	Value
Propellant Type	Kind of Propellant	-	UDMH/ N_2O_4
Thrust (S.L.)	Performance	kN	1474
Thrust (Vac.)	Performance	kN	1635
Specific Impulse (S.L.)	Performance	s	285.2
Specific Impulse (Vac.)	Performance	s	316.3
Chamber Pressure	Performance	bar	147
Exit Pressure	Performance	bar	0.6
Ambient Pressure	Ambient pressure	bar	0.6
Dry Mass	Performance	kg	1280
Burning Time	Performance	s	130
Max. Nozzle Diameter	Dimension	mm	1500

Archive of SID.ir

Archive of SID.ir

3. The Design Variables and the Objective Functions

There are five steps to present the new hybrid meta-model with the DOE and RSM. These steps are considered as follows: selecting the experiment design; conducting the experiment; defining the optimization problem; validating the optimal values; and conclusions and suggestions. To this end, Figs. (3) and (4) show the feed system optimization algorithm based on the DOE and the feed system optimization algorithm based on a hybrid meta-model, respectively. Each of the steps of the hybrid meta-model approach is explained in the following.

In the DOE and the RSM, words providing specific definitions of this technique are often used. Hence, each word and its applications in this study are briefly described below.

Variable: Variables are elements that are measured and form the basis for these experiments. Some of these variables include the oxidizer path input pressure and the turbine efficiency (Table (2)).

Response variable: A response variable is a variable that shows the ultimate output or state. The response variables reflect the system performance. In this study, the response surface variable is the power-to-mass ratio of the feed system (Table 3).

Mutual effects: The change simultaneously made by two or several variables in the response variable.

Table 2. The input variables of the upper and lower surfaces of the feed system.

Design Function	Requirements	Nominal Value	Min.	Max.	Notation	Units
System	Input Pressure of Oxidizer Pump	3	2.5	5	P_in_ox	bar
System	Input Pressure of Fuel Pump	3	2.5	5	P_in_fu	bar
Pre-burner	Pre-burner Temperature	800	700	900	T_gg	K
Turbine	Turbine Efficiency	0.74	0.7	0.85	Eta_tr	-
Turbine	Rotational Speed	13800	12500	15000	Rev.	rpm
Main Oxidizer Pump	Pump Efficiency	0.7	0.65	0.8	Eta_ox_pu	-
Pre-burner Kick Pump	Inlet Relative Cross-Section Area	0.3	0.25	0.4	IRCSA	-

Table 3. The feed system's objective function.

Response	Name	Nominal Value	Notation	Units
R1	Power to mass ratio of the feeding system	71	N/M	kW/kg

Table 4. A summary of the information on the input variables in the Meta-Model method.

Factor	Name	Units	Type	Min	Max	Coded Low	Coded High	Mean	Standard Deviation
A	P_in_ox	bar	Numeric	2.50	5.00	-1 ↔ 2.50	+1 ↔ 5.00	3.75	0.7841
B	P_in_fu	bar	Numeric	2.50	5.00	-1 ↔ 2.50	+1 ↔ 5.00	3.75	0.7841
C	T_gg	K	Numeric	700	900	-1 ↔ 700	+1 ↔ 900	800	62.73
D	Eta_tr	-	Numeric	0.7000	0.8500	-1 ↔ 0.70	+1 ↔ 0.85	0.7750	0.0470
E	Rev.	rpm	Numeric	12500	15000	-1 ↔ 12500	+1 ↔ 15000	13750	784.06
F	Eta_ox_pu	Eta_ox_pu	Numeric	0.6500	0.8000	-1 ↔ 0.65	+1 ↔ 0.80	0.7250	0.0470
G	IRCSA	-	Numeric	0.2500	0.4000	-1 ↔ 0.25	+1 ↔ 0.40	0.3250	0.0470

Archive of SID.ir

Archive of SID.ir

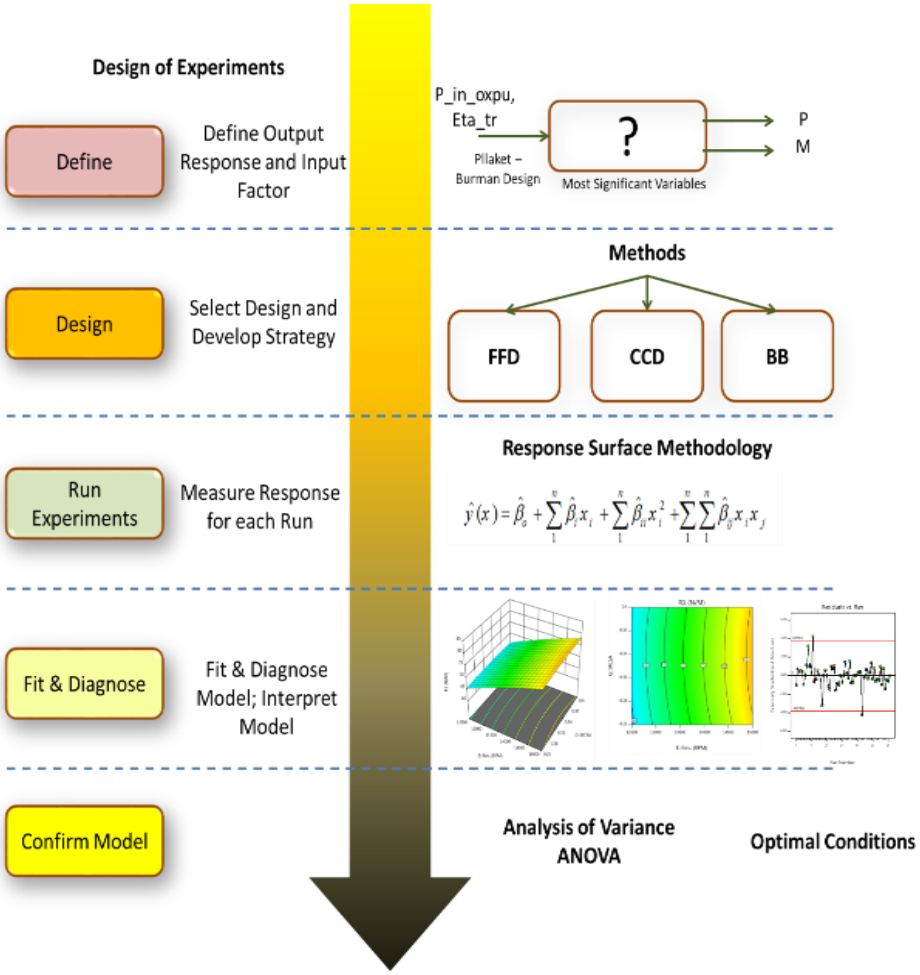

Fig.3. The feed system optimization algorithm based on the DOE.

Table 5. The different data values of the experiment variables and the responses

		Factor1	Factor2	Factor3	Factor4	Factor5	Factor6	Factor7	Output1	Output2	Response
Row	Run	A: P_in_ox	B: P_in_fu	C: T_gg	D: Eta_tr	E: Rev.	F: Eta_ox_pu	G: IRCSA	Power	mass	R1
		Bar	bar	K	-	rpm	-	-	kw	kg	kw/kg
1	49	3.75	3.75	800	0.7	12500	0.65	0.325	17624	255	69.1
2	60	3.75	3.75	800	0.85	12500	0.65	0.325	16986	244	69.6
3	24	3.75	3.75	800	0.7	15000	0.65	0.325	17624	215	81.9
4	13	3.75	3.75	800	0.85	15000	0.65	0.325	16986	206	82.4
5	47	3.75	3.75	800	0.7	12500	0.8	0.325	15167	248	61.1
6	1	3.75	3.75	800	0.85	12500	0.8	0.325	14752	239	61.7
7	5	3.75	3.75	800	0.7	15000	0.8	0.325	15167	210	72.2
8	51	3.75	3.75	800	0.85	15000	0.8	0.325	14752	202	73.0
9	15	2.5	3.75	800	0.775	13750	0.65	0.25	17450	230	75.8
10	20	5	3.75	800	0.775	13750	0.65	0.25	17318	228	75.9

Archive of SID.ir

Archive of SID.ir

4. The Developed Hybrid Meta-Model Methodology Implementation

In this phase, the CCD structure dedicated several 64 experiments that were performed in the design code. Table (5) shows some of the experiment results.

4.1. Data Analysis

Data analysis must be interpreted based on the existing engine data; in case the data comparison must be performed between the existing data and the meta-model, that can help conceptually to designer to conceive the reasons for differences. There are numerous useful software packages for data analysis, while the graphic-based methods play a significant role in data analysis and in predicting the system behavior. The residual analysis and assessment tool of the model quality is also among the important analysis tools. The prediction of residual analysis leads to predicting the truncated error in the meta-model. The statistical methods adopted in the DOE include the examination of hypotheses, calculation of diagrams, analysis of variance, and regression analysis. The results of the performed experiments results were entered into the design code thereafter. After several steps, the code calculates the different states of the RSM and introduces the most suitable state based on the R^2 and $R^2_{Adjusted}$ (Table (6)). As seen, the code suggests the quadratic state for this problem. Table (7) shows the objective function in the quadratic state. The ANOVA for quadratic state is shown in Table (8). Four parameters (Pre-burner Temperature, Turbine Efficiency, Rotational speed, and Pump efficiency) have the most impact on the objective function.

The behavior of the residuals versus the predictions in different iterations is illustrated in Fig. (5). As seen, almost the whole of the experiments are between two horizontal red lines, reflecting the high precision of the model. Similarly, in Fig. (6), which presents the Box–Cox diagram of the metamorphosis power, if the blue line comes in between the two red lines, there is no need for the transition equations.

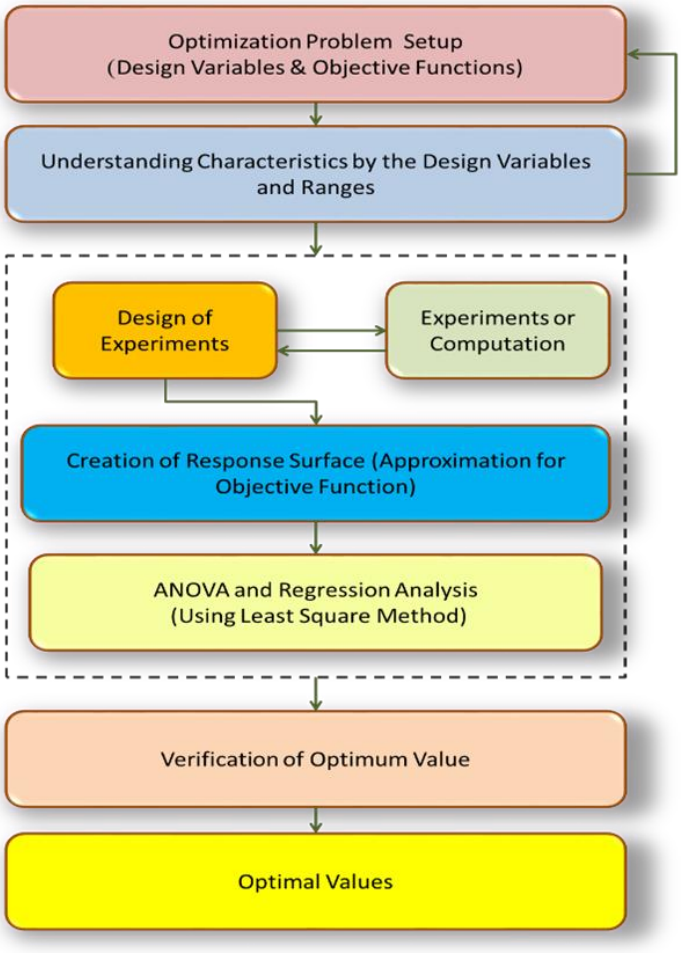

Fig.4. The feed system optimization algorithm based on the new hybrid metal mode.

Archive of SID.ir

Archive of SID.ir

Table 6. The different sources of Cubic, Quadratic, 2FI, and Linear.

Source	Standard Deviation	R^2	R^2 Adjusted	PredictedR^2	PRESS	state
Linear	0.7140	0.9797	0.9771	0.9729	36.70	
2FI	0.8703	0.9816	0.9659	0.9258	100.51	
Quadratic	0.2453	0.9988	0.9973	0.9918	11.13	**Suggested**
Cubic	0.0000	1.0000	1.0000	-	*	Aliased

Table 7. The objective function in the Quadratic State.

Response	Units	Observations	Min	Max	Mean	standard Deviation	Transform	Model
R1	N/M	62	61.1573	82.4563	71.75	4.71	None	**Quadratic**

Table 8. The ANOVA for Quadratic State.

Source	Sum of Squares	df	Mean Square	F-value	p-value	State
	1353.73	35	38.68	642.69	< 0.0001	-
A-P_in_ox	0.1611	1	0.1611	2.68	0.1138	-
B-P_in_fu	0.0871	1	0.0871	1.45	0.2397	-
C-T_gg	4.15	1	4.15	69.02	< 0.0001	**Significant**
D-Eta_tr	3.60	1	3.60	59.79	< 0.0001	**Significant**
E-Rev.	861.82	1	861.82	14320.32	< 0.0001	**Significant**
F-Eta_ox_pu	457.80	1	457.80	7606.97	< 0.0001	**Significant**
G-IRCSA	0.1413	1	0.1413	2.35	0.1375	-
AB	8.760E-06	1	8.760E-06	0.0001	0.9905	-
AC	0.0078	1	0.0078	0.1302	0.7212	-
AD	0.0006	1	0.0006	0.0096	0.9229	-
AE	0.0423	1	0.0423	0.7031	0.4094	-
AF	0.0125	1	0.0125	0.2073	0.6527	-
AG	0.0499	1	0.0499	0.8290	0.3709	-
BC	0.0075	1	0.0075	0.1247	0.7268	-
BD	0.0588	1	0.0588	0.9777	0.3319	-
BE	0.0247	1	0.0247	0.4101	0.5275	-
BF	0.0068	1	0.0068	0.1132	0.7393	-
BG	0.0000	1	0.0000	0.0000	1.0000	-
CD	0.1178	1	0.1178	1.96	0.1736	-
CE	0.0005	1	0.0005	0.0090	0.9252	-
CF	0.0151	1	0.0151	0.2508	0.6207	-
CG	0.0178	1	0.0178	0.2963	0.5908	-
DE	0.0062	1	0.0062	0.1028	0.7510	-
DF	0.0187	1	0.0187	0.3115	0.5816	-
DG	0.7647	1	0.7647	12.71	0.0014	-
EF	1.38	1	1.38	23.00	< 0.0001	**Significant**
EG	0.0000	1	0.0000	0.0000	1.0000	-
FG	0.0001	1	0.0001	0.0013	0.9714	-
A^2	1.67	1	1.67	27.77	< 0.0001	**Significant**
B^2	2.12	1	2.12	35.16	< 0.0001	**Significant**
C^2	7.12	1	7.12	118.29	< 0.0001	**Significant**
D^2	4.75	1	4.75	78.91	< 0.0001	**Significant**
E^2	2.35	1	2.35	39.07	< 0.0001	**Significant**
G^2	3.93	1	3.93	65.38	< 0.0001	**Significant**

Archive of SID.ir

Archive of SID.ir

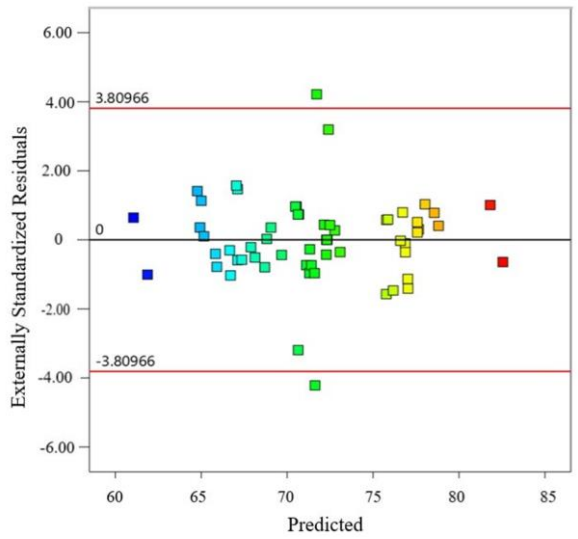

Fig. 5. The behavior of the residuals versus the predictions.

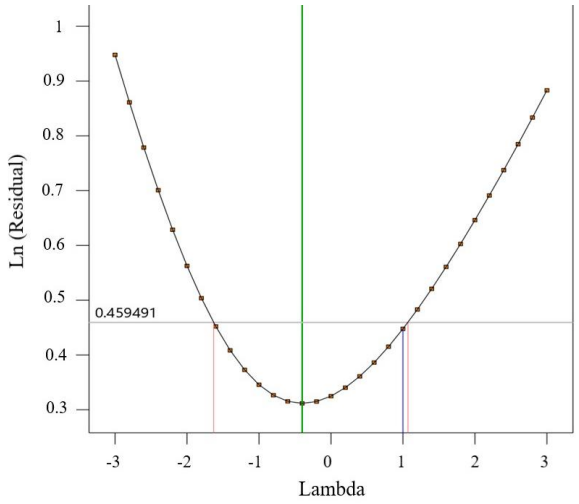

Fig. 6. The Box–Cox diagram of the metamorphosis power.

4.2. The Response Surface Equation (RSE)

A mathematical model is built up to identify the correlation between design variables and select the significant variables. The mutual interactions of these design variables are mapped in the design space by RSM and variation contour plots. The RSE which is derived based on the seven input design variables shown in Table (2). The RSE predicts the behavior of the objective functions, the power to mass ratio of the feed system in terms of the surfaces of given by each design variable. To predict the model behavior, for the objective function, it is sufficient to number in the relevant equations instead of the design variables. It is observed that RSE predicts solutions with an error of less than 2%. Another important result that can be derived from the RSE is the investigation of the effect of variables on the objective function.

4.3. Analysis of the RSM

The behavior of the objective function relative to two input design variables is illustrated in Figs. (5) to (9). In the graph analyses, when the behavior of the objective function is analyzed relative to two design variables, the other design variables are considered constant. As seen, the range of variations of the objective function is between 61.1573 and 82.4563. In all Figures, the upper response surface curve and the lower curve represent the behaviors of two design variables with a constant objective function. In Fig. (7), the response surface curve for the two design variables, the fuel pump input pressure and the oxide pump efficiency, is shown. It is observed that, in order to constant response, as the fuel pump input pressure increases, the oxide pump efficiency first increases and then decreases. Alternatively, with a constant fuel pump input pressure, as the oxide pump efficiency increases, the response reduces.

As seen in Fig. (8), the response surface curve for the two design variables, the turbine efficiency and Pre-burner Temperature, is illustrated. It is observed that there is no direct relationship between these two design variables. In Fig. (9), the response surface curve for the two design variables, turbine efficiency and turbine revolution, is shown. It is considered that, in order to constant response, as turbine efficiency increases, turbine revolutions decrease. On the other hand, with a constant turbine efficiency, in order to increase the objective function, the turbine revolution must be increased. As seen in Fig. (10), the response surface curve for the two design variables, Pre-burner Temperature and turbine revolution, is illustrated. It is observed that, in order for the objective function to remain constant, as Pre-burner Temperature increases, turbine revolutions are reduced. Alternatively, with a constant Pre-burner temperature, as turbine revolution increases, the response is enhanced. The increased Pre-burner Temperature reduces the overall power and mass at a constant turbo-pump revolution. This outcome sounds unusual at first, but a deeper analysis reveals the accuracy of this relationship. Since the pre-burner is rich in oxidizer, the flow rate of the oxidizer has to be reduced to increase the

Archive of SID.ir

Archive of SID.ir

temperature. Furthermore, $N_{Tr} \propto \sqrt{RT} * \dot{m}$ The turbine power changes proportionally to $\sqrt{RT}$ and has a direct relationship with consumption. Besides, the $\dot{m}$ the effect is the dominant effect in increasing or reducing the turbo-pump effect. Hence, the turbine power decreases due to a decrease in consumption, despite the increase in temperature.

In Fig. (11), the response surface curve for the two design variables, turbine revolution and oxidizer pump efficiency, is shown. It is considered that, in order to maintain constant, as the oxidizer pump efficiency increases, the turbine revolution increases. On the other hand, with a constant turbine revolution, in order to increase the objective function, the turbine revolution must be increased.

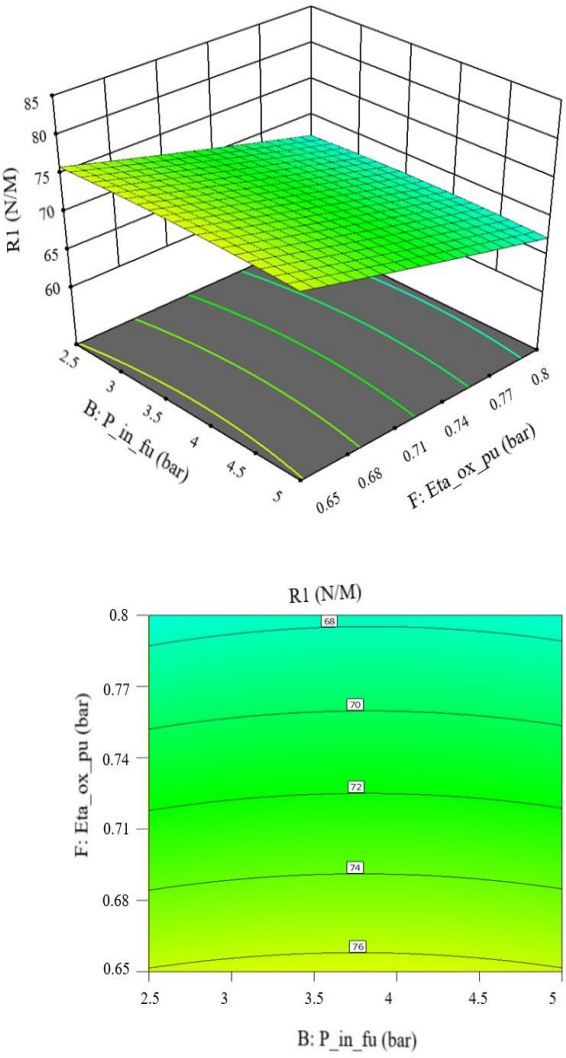

Fig. 7. The surface response curve for two design variables, namely the fuel pump input pressure and the oxide pump efficiency.

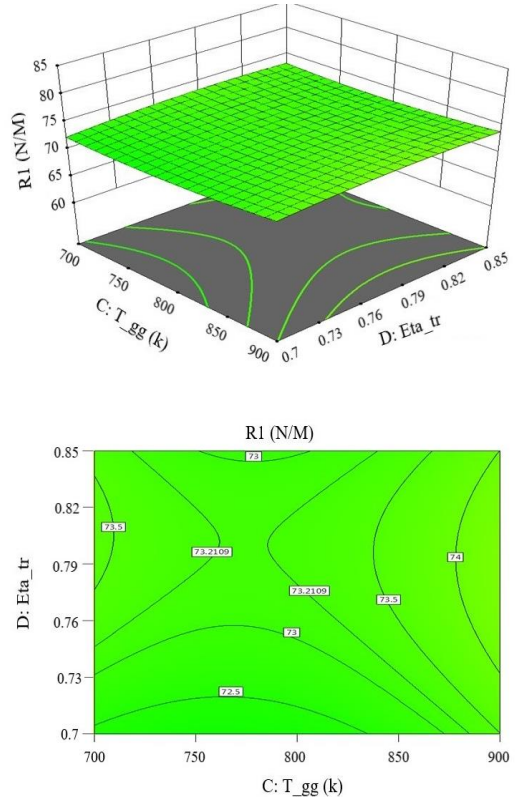

Fig. 8. The surface response curve for the turbine efficiency and Pre-burner Temperature.

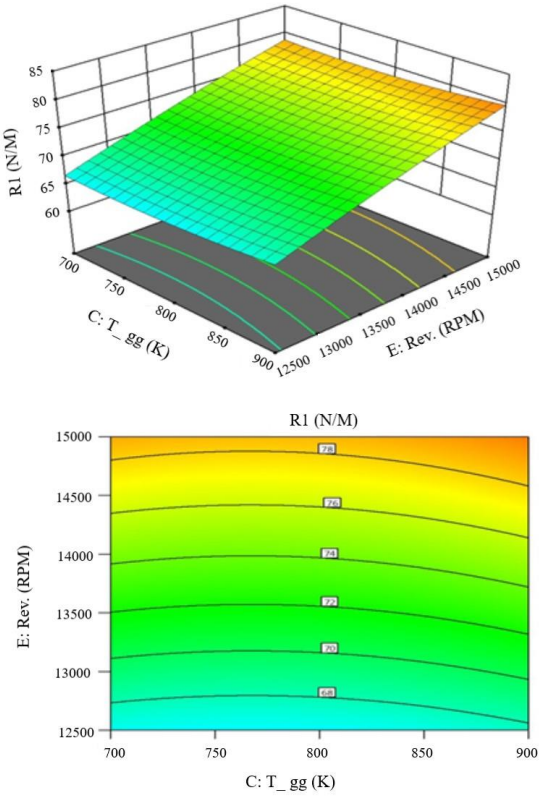

Fig. 9. The surface response curve for the turbine revolutions per minute and turbine efficiency design variables.

Archive of SID.ir

Archive of SID.ir

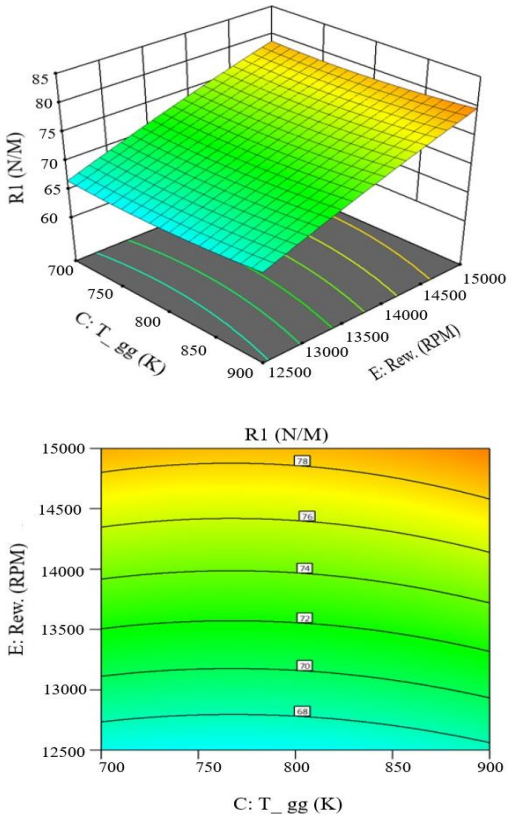

Fig. 10. The surface response curve for the turbine revolutions per minute and Pre-burner Temperature design variables.

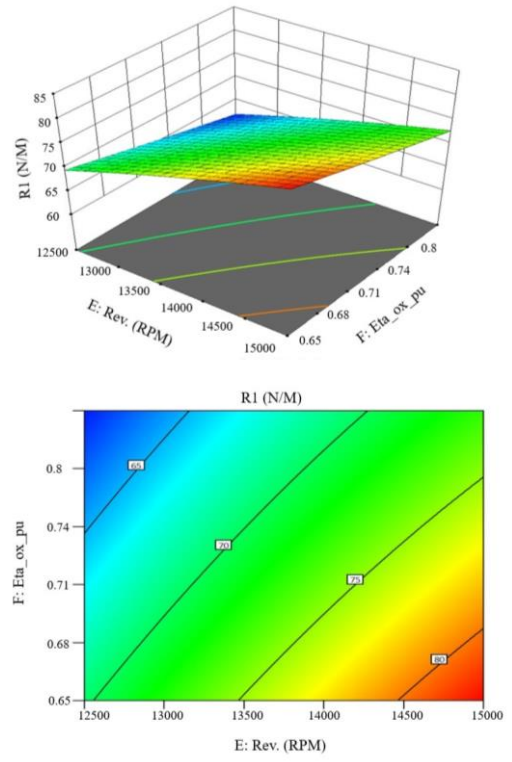

Fig. 11. The surface response curve for the oxidizer pump efficiency and turbine revolutions per minute design variables.

5. THE FEED SYSTEM OPTIMIZATION BY NEW HYBRID META-MODEL METHODOLOGY

Design optimization refers to the process of finding a logical design that is the best possible design for the attainment of a given objective by considering the geometrical and operating constraints. With a realistic approach, it could be stated that design optimization is a systematic method of improving designs. The optimization section in a statistical program searches for a combination of factor levels that simultaneously satisfy the requirements placed on each of the responses and factors. Furthermore, this optimization technique searches the design space, using the developed mathematical model to find the factor settings that optimize any combination of one or more objective functions. The objective functions are combined into an overall desirability function. This optimization methodology will be able to find a point that maximizes or minimizes the desirability function. In the criterion, the objective functions are set to simultaneously maximize the produced power and minimize the system weight. To this end, the process parameters are kept within the range of the studied design space. Table (9) shows the adjustment of parameters for optimization. Table (10) illustrates the criteria, representing the objective functions, upper and lower limits, as well as the importance of each objective function for each response and factor. Tables (10) to (14) show the pre-optimization information, the post-optimization test factors, and the post-optimization surface response. Table (14) shows the results of the best seven combination sets of Pareto optimal parameters for selected criteria. It is evident from the results that to achieve the optimum objective function, the parameters are as follows:

- The input pressure of the oxidizer pump has to be 4.997,
- Input pressure of the fuel pump has to be 2.636,
- Pre-burner temperature has to be 878,
- Turbine efficiency has to be 0.848,
- Rotational speed has to be 14953,
- Pump efficiency has to be 0.65 and
- The Inlet Relative Cross-Section area has to be 0.33.

5.1. Verification test

The results of optimization have been obtained by desirability function analysis and also validated by conducting confirmatory tests. Confirmatory tests have been conducted in RPA software and achieved the experiments. The tested results of experiments at

Archive of SID.ir

Archive of SID.ir

optimum conditions are presented in Table (15). It is obtained from Table (14) that there is a small error percentage between the optimum and the experimental values, which validates the applied optimization technique. As can be seen from Table (14), at the selected point with desirability equal to 1, the value of the objective function (Power/Weight ratio) is 82.491. The value in Table (15) after applying the new hybrid meta-model is 81. This small error means high accuracy of the developed meta-model

Table 9. The software input parameters for optimization.

Optimization Option	Value
Random Starting Points	3000
Number Of Design Points	90
Duplicate Solution Filter	0.5
Simplex Fraction	0.1
Maximum Number of Solutions	300

Table 10. The design constraints in the feed system optimization.

Number	Name	Objective	Lower Limit	Upper Limit	Lower Weight	Upper Weight
1	A: P_in_ox	is in range	2.5	5	1	1
2	B: P_in_fu	is in range	2.5	5	1	1
3	C: T_gg	is in range	700	900	1	1
4	D: Eta_tr	is in range	0.7	0.85	1	1
5	E: Rev.	is in range	12500	15000	1	1
6	F: Eta_ox_pu	is in range	0.65	0.8	1	1
7	G: IRCSA	is in range	0.25	0.4	1	1
8	R1	maximize	61.1573	82.4563	1	1

Table 11. Part of the solutions found for the four design variables and surface responses in the feed system optimization.

Number	Eta_ox_pu	Eta_tr	T_gg	P_in_ox	R1	Desirability
1	0.651	0.848	878	4.997	82.491	1.000
2	0.651	0.820	879	3.705	82.663	1.000
3	0.651	0.786	720	4.500	82.460	1.000
4	0.650	0.762	737	4.679	82.518	1.000
5	0.650	0.718	899	4.810	82.457	1.000
6	0.651	0.827	874	3.710	82.765	1.000
7	0.650	0.828	750	4.137	82.473	1.000
8	0.650	0.720	827	4.355	82.457	1.000
9	0.657	0.791	881	3.013	82.471	1.000
10	0.654	0.737	895	3.927	82.650	1.000

Table 12. The test factors in the post-optimization analysis of the feed system.

Factor	**Name**	**Level**	**Low Level**	**High Level**	**Standard deviation**	**Coding**
A	P_in_ox	4.65	2.50	5	0	Actual
B	P_in_fu	3.16	2.50	5	0	Actual
C	T_gg	713.28	700.00	900	0	Actual
D	Eta_tr	0.8221	0.7000	0.85	0	Actual
E	Rev.	14982.40	12500.00	1500	0	Actual
F	Eta_ox_pu	0.6532	0.6500	0.8	0	Actual
G	IRCSA	0.2903	0.2500	0.4	0	Actual

Archive of SID.ir

Archive of SID.ir

Table 13. The statistical information of the quadratic surface response.

Response	Predicted Mean	Standard Deviation	SE Mean	95% CI low for Mean	95% CI high for Mean	95% TI low for 99% Pop	95% TI high for 99% Pop
R1	82.4889	0.24532	0.253346	81.9681	83.0096	81.2304	83.7474

Table 14. The output of the search for the optimum.

Number	P_in_ox	P_in_fu	T_gg	Eta_tr	Rev.	Eta_ox_pu	IRCSA	Objective function (R1)	Desirability	
1	4.997	2.636	878.303	0.848	14953.963	0.651	0.330	82.491	1.000	**Selected**
2	3.705	2.575	879.412	0.820	14897.211	0.651	0.311	82.663	1.000	
3	4.500	3.923	720.664	0.786	14913.153	0.651	0.320	82.460	1.000	
4	4.679	3.441	737.071	0.762	14995.704	0.650	0.308	82.518	1.000	
5	4.810	4.665	899.635	0.718	14998.254	0.650	0.273	82.457	1.000	
6	3.710	3.468	874.607	0.827	14983.733	0.651	0.389	82.765	1.000	
7	4.137	2.874	750.354	0.828	14994.717	0.650	0.296	82.473	1.000	
8	4.355	3.739	827.450	0.720	14999.119	0.650	0.340	82.457	1.000	
9	3.013	3.727	881.262	0.791	14887.427	0.657	0.335	82.471	1.000	
10	3.927	4.458	895.386	0.737	14906.297	0.654	0.385	82.650	1.000	

Table 15. Comparing the operating characteristics of the existing engine and the engine optimized with the new hybrid meta-model method

Existing Engine (RD-253)	Optimized Engine
Engine performance	**Engine performance**
specific impulse (vac.): 314.26 s	specific impulse (vac.): 314.26 s
specific impulse (SL): 279.60 s	specific impulse (SL): 279.60 s
thrust (vac.): 1577.22 kN	thrust (vac.): 1577.22 kN
thrust (SL): 1403.28 kN	thrust (SL): 1403.28 KN
Power Subsystem	**Power Subsystem**
Power: 16265 kw	Power: 16293 kw
turbopump/s: 226.85 kg	turbopump/s: 201.16 kg
Power/Weight: 71.7	Power/Weight: 81
Engine dry mass estimation	**Engine dry mass estimation**
chamber/s: 736.74 kg	chamber/s: 736.74 kg
turbopump/s: 226.85 kg	turbopump/s: 201.16 kg
other components: 369.10 kg	other components: 369.10 kg
total: 1332.69 kg	total: 1307.00 kg
Thrust-to-Weight ratio estimation	**Thrust-to-Weight ratio estimation**
in vacuum: 120.68	in vacuum: 123.05
at sea level: 107.37	at sea level: 109.48

Archive of SID.ir

Archive of SID.ir

6. CONCLUSIONS

In the present study, a new hybrid meta-model by using DOE and RSM has been developed. The developed model has been applied to optimize the LPE's feed system. To this end, the mathematical model has been derived and performed multi-response optimization of the feed system. From the foregoing analysis and discussion, the following conclusions have been drawn:

1) The developed second-order RSE can predict the values of the feed system characteristics with high accuracy. The developed empirical model has been tested by ANOVA with a confidence level of 95%.
2) The optimized parameters in this optimization problem are input pressure of oxidizer pump, input pressure of fuel pump, pre-burner temperature, turbine efficiency, rotational speed, pump efficiency, and inlet relative cross-section area, and the results have been validated by using a confirmatory test.
3) The increased pre-ignition temperature in the engine reduces the overall power and mass at a constant turbo-pump rpm (revolutions per minute).
4) The percentage error between the new hybrid meta-model and the confirmatory result is found to be approximately ~2%, which validates when applied to the existing LPE's feed system (RD-253).
5) The four parameters, pre-burner temperature, turbine efficiency, rotational speed, and pump efficiency, have the most impact on the objective function (power/weight ratio).
6) The three parameters, input pressure of oxidizer pump, input pressure of fuel pump, and inlet relative cross-section area, have the least impact on the objective function (power/weight ratio).
7) The difference between the optimal in the objective function results is less than 2%, which confirms the high precision of the new hybrid meta-model.
8) The "thrust-to-weight" ratio can be optimized by up to 2%.

A comparison between the optimized LPE's feed system and the existing LPE's feed system indicates that the existing feed system can be optimized by up to 13 %.

Nomenclature

P_in_ox	**Input Pressure of Oxidizer Pump (bar)**
P_in_fu	Input Pressure of Fuel Pump (bar)
T_gg	Pre-burner Temperature (K)
Eta_tr	Turbine Efficiency (-)
Rev.	Rotational Speed (rpm)
Eta_ox_pu	Pump Efficiency (-)
IRCSA	Inlet Relative Cross-Section area (m^2)
R1	Power to mass ratio of the feeding system (kW/kg)
CI	confidence interval
95% CI	95% of confidence intervals generated from similar independent experiments will contain the actual average outcome for the current factor settings.
TI	tolerance interval
95% TI	95% of tolerance intervals generated from similar independent experiments will contain X% of all future observations for the current factor settings, where X is between 0 and 100.
GA	Genetic Algorithm
RPA	Rocket Propulsion Analysis
R^2	R-Squared
adjusted R^2	A measure of the amount of variation about the mean explained by the model.
PRESS	The Predicted Residual Sum of Squares for the model
2FI	2-factor interactions
df	Degree of freedom
F-value	**The F value is used in the variance analysis.**

CONFLICT OF INTEREST

The authors of this paper declared no conflict of interest regarding the authorship or publication of this article.

REFERENCES

[1] G. P. Sutton and O. Biblarz, *Rocket Propulsion Elements*, 8nd ed. New York: John Wiley & Sons, 2010.

Archive of SID.ir

Archive of SID.ir

[2] M. Son, J. Koo, W. Cho, and E. S. Lee, "Conceptual design for a kerosene fuel-rich gas-generator of a turbo-pump-fed liquid rocket engine," *Journal of Thermal Science*, vol. 21, pp. 428-434, 2012, https://doi.org/10.1007/s11630-012-0564-z.

[3] K. S. Jeon, J. W. Lee, C. Lee, and J. W. Chang, "Optimal gas generator design for the liquid rocket engine," in *42th AIAA Aerospace Sciences Meeting and Exhibit*, Reno, Nevada, Peper 2004-32, 2004, https://doi.org/10.2514/6.2004-32.

[4] H. Burkhardt, M. Sippel, A. Herbertz, and J. Klevanski, "Comparative study of kerosene and methane propellant engines for reusable liquid booster stages," in *4th International Conference on Launcher Technology "Space Launcher Liquid Propulsion*", Liège, Belgium, 2002.

[5] D. R. Jones, "Multivariable optimization of liquid rocket engines using particle swarm algorithms," M. S. thesis, Aerospace Engineering and Mechanics in the Graduate School of The University of Alabama, United States. 2013.

[6] A. Butt, C. G. Popp, H. M. Pitts, and D. J. Sharp, "NASA ares i launch vehicle roll and reaction control systems design status," in *45th AIAA/ASME/SAE/ASEE Joint Propulsion Conference &Exhibit*, Denver, Colorado, 2008, Peper 5130, https://doi.org/10.2514/6.2009-5130.

[7] M. Kanazaki, A. Ariyairt, K. Chiba, K. Kitagawa, and T. Shimada, "Conceptual design of single-stage rocket using hybrid rocket by means of genetic algorithm," *Procedia Engineering*, vol. 99, pp. 198-207, 2015, https://doi.org/10.1016/j.proeng.2014.12.526.

[8] D. W. Way and J. R. Olds, "SCORES: web-based rocket propulsion analysis tool for space transportation system design," in *35th AIAA/ASME/SAE/ASEE Joint Propulsion Conference*, Los Angeles, CA, 1999.

[9] J. D. Shelton, R. A. Frederick, and A. W. Wilhite, "Launch vehicle propulsion design with multiple selection criteria", *Journal of Spacecraft Rockets*, vol. 43, no. 4, pp. 893–902, 2006, https://doi.org/10.2514/1.16919.

[10] A. Saqlain and H. Lin-shu, "Optimization and sizing for propulsion system of liquid rocket using genetic algorithm," *Chinese Journal of Aeronautics*, vol. 20, no. 1, pp. 40–46, 2007, https://doi.org/10.1016/S1000-9361(07)60005-3.

[11] M. Shafaee, P. Mohammad Zadeh, A. Elkaie, and H. Fallah, "Design optimization of a thrust chamber using a mass-based model to improve the geometrical and performance parameters of low-thrust space propulsion systems," *Proceedings of the Institution of Mechanical Engineers, Part G: Journal of Aerospace Engineering*, vol. 233, no. 5, pp. 1820-1837, 2018, https://doi.org/10.1177/0954410018767288.

[12] X. B. lam, "Multidisciplinary design optimization for aircraft wing using response surface method, genetic algorithm, and simulated annealing," *Journal of Science and Technology in Civil Engineering (JSTCE)-HUCE*, vol. 14, no. 1, pp. 28-41, 2020, https://doi.org/10.31814/stce.nuce2020-14(1)-03.

[13] N. Soldà and D. Lentini, "Opportunities for a liquid rocket feed system based on electric pumps," *Journal of Propulsion and Power*, vol. 24, no. 6, pp. 31340-1346, 2008, https://doi.org/10.2514/1.35074.

[14] P. A. Pavlov Rachov, H. Tacca, and L. Lentini, "Electric feed systems for liquid-propellant rockets", *Journal of Propulsion and Power*, vol. 29, no. 5, pp. 1171-1180, 2013, https://doi.org/10.2514/1.B34714.

[15] S. A. Moussavi Torshizi, A. Hajilouy Benisi, and M. Durali, "Multi-level optimization of the splitter blade profile in the impeller of a centrifugal compressor," *Journal of Scientia Iranica Transactions B: Mechanical Engineering*, vol. 24, no. 2, pp. 707-714, 2017.

[16] M. Mojaddam and K. R. Pullen, "Optimization of a centrifugal compressor using the design of experiment technique," *Applied Science*, vol. 9, no. 2, 2019, Art. no. 291, https://doi.org/10.3390/app9020291.

[17] L. Lei, H. Wan, W. Gao, F. Tong, and H. Li, "Reliability-based multidisciplinary design optimization of cooling turbine blade considering uncertainty data statistics," *Structural and multidisciplinary optimization*, vol. 29, pp. 659-673, 2019, https://doi.org/10.1007/s00158-018-2081-5.

COPYRIGHTS

Authors retain the copyright and full publishing rights.
Published by Iranian Aerospace Society. This article is an open access article licensed under
The Creative Commons Attribution 4.0 International (CC BY 4.0).

HOW TO SITE THIS ATRICLE

H. R. Alimohammadi, H. Naseh, and F. ommi, "The New Hybrid Meta-Model by Using DOE and RSM for Liquid Propellant Engine's Feed System Optimization," *Journal of Aerospace Science and Technology*, Vol. 17, Issue 2, 2024, pp. 110-124.
DOI: https://doi.org/10.22034/jast.2023.367044.1135
URL: https://jast.ias.ir/article_186102.html

Archive of SID.ir